

Supporting Information for:

**A series of novel Co(II)-based MOFs: Syntheses, structures, and diversity
properties**

Yaoyi Wei, Bin Zhu, Jinmiao Wang, Lulu Wang, Ruixue Wu, Wenbo Liu, Bingxiang Ma, Dong Yang,

Yuhua Fan**, Xia Zhang*

Key Laboratory of Marine Chemistry Theory and Technology, Ministry of Education, College of Chemistry and Chemical
Engineering, Ocean University of China, Qingdao, Shandong, 266100, PR China

Corresponding author: Xia Zhang

E-mail: zhangxiaouc@163.com

Text S1. Materials and general measurements, syntheses of MOFs **1-3**.

Text S2. Adsorption isotherms.

Text S3. Adsorption kinetics models.

Text S4. Adsorption thermodynamic parameters.

Table S1. Selected bond lengths (Å) and angles (°) for MOFs **1-3**.

Fig. S1. TG curve of MOFs **1-3**.

Fig. S2. The PXRD patterns of **1-3** before and after adsorption.

Fig. S3. Naked eye visualization of the adsorption of 100 ppm CR by **1** at room temperature and the corresponding UV-vis spectra of the solution.

Fig. S4. The repeated adsorptions of CR for **1**.

Fig. S5. Van't Hoff plots for the adsorption of CR dye onto **1**.

Fig. S6. Structural formula of congo red.

Fig. S7. The PXRD patterns of **1-3** before and after electrocatalysis.

Text S1. Materials and general measurements, syntheses of MOFs 1-3.

3-(3,5-dicarboxylphenoxy)pyridine = H₂L; 3,5-bis(1-imidazolyl)pyridine = bip; 4,4'-bis(imidazol-1-yl)biphenyl = bibp; 1,1'-(1,4-butanediyl) bis (imidazole) = bbi were purchased from Jinan Henghua Sci. & Tec. Co. Ltd. Co(NO₃)₂·6H₂O, congo red (CR), fluorescein sodium (NaFL), acriflavine hydrochloride (AH), orange G (OG), orange II (OII), methylene blue (MB), methyl violet (MV), ethanol, acetonitrile, dimethylformamide (DMF) were obtained from Aladdin Chemistry Co, Ltd, China. All reagents in the course of the experiment were analytical grade and could be used without further purification.

The X-ray diffraction (XRD) patterns were performed on a D/max 2200 vpc diffractometer (Rigaku Corporation, Japan) with the Cu-K α radiation. The powder X-ray diffractions (PXRD) were collected on an Enraf-Nonius CAD-4 X-ray single-crystal diffractometer with Cu-K α radiation. Elemental analyses (C, H, N) were performed in a model 2400 PerkinElmer analyzer. Dye concentrations were tested by spectrophotometer (Shanghai Yuanxi, UV-1250). Infrared spectra in the 4000-400 cm⁻¹ region were recorded on a Nicolet 170SX spectrometer using KBr powder. Thermogravimetric analyses (TGA) were measured on a Perkin-Elmer TGA-7, thermogravimetric analyzer under air conditions from room temperature to 900 °C with a heating rate of 10 °C·min⁻¹. Cyclic voltammetry curves were measured by CHI660e electrochemical workstation (from Shanghai Chenhua). Zeta potential was measured by a zeta analyzer (Marven, Nano-ZS90). X-ray Photoelectron Spectroscopy (XPS) were tested by Thermo, ESCALAB 250Xi. Topological analyses were performed and confirmed by the Topos program and the Systre software. The magnetic susceptibility measurements of the samples were carried out with MPMS-XL-7 magnetometer (from Quantum Design).

Synthesis of {[Co₃(L)₃(bip)]·2H₂O}_n (1)

A mixture of Co(NO₃)₂·6H₂O (0.031g, 0.1 mmol), H₂L (0.026 g, 0.1 mmol) bipd (0.021 g, 0.1 mmol), Acetonitrile (5 mL) and H₂O (5 mL) were stirred for 0.5 hour in air. And then the solution was transformed into the Teflon-lined stainless steel vessel (15 mL), sealed and heated to 130 °C and kept for 3 days. Subsequently, the vessel was cooled to the room temperature at the degree of 5 °C·h⁻¹. Purple block crystals were collected with the yield of 71.5 % (based on cobalt). Anal. Calcd for C₅₀H₃₀Co₃N₈O₁₅: C, 51.78; H, 2.59, N, 9.67 %. Found: C, 51.73; H,

2.73; N, 9.16 %. IR (KBr disk, cm^{-1}): 3430 (m), 3137 (w), 1618 (vs), 1561 (s), 1511 (w), 1459 (w), 1392 (vs), 1313 (w), 1270 (w), 1186 (w), 975 (w), 783 (m), 723 (m), 655 (w).

Synthesis of $[\text{Co}(\text{L})(\text{bibp})_{0.5}]_n$ (**2**)

Changing the bip of **1** to bibp (0.029 g, 0.1 mmol) and the solvent to Dimethylformamide (6 mL) and H_2O (2 mL), other conditions remained unchanged. Pink block crystals were collected with the yield of 85.7 % (based on cobalt). Anal. Calcd for $\text{C}_{22}\text{H}_{14}\text{CoN}_3\text{O}_5$: C, 53.30; H, 2.83, N, 8.48 %. Found: C, 53.15; H, 2.95; N, 8.33 %. IR (KBr disk, cm^{-1}): 3437 (m), 3114 (w), 1626 (s), 1551 (s), 1518 (m), 1514 (m), 1462 (w), 1386(vs), 1318 (w), 1265 (s), 1070 (m), 876 (m), 818 (m), 734 (s), 538 (w), 436 (w).

Synthesis of $[\text{Co}(\text{L})(\text{bbi})_{0.5}]_n$ (**3**)

Changing the bip of **1** to bbi (0.019 g, 0.1 mmol), and the solvent to Dimethylformamide (5 mL) and H_2O (5 mL), other conditions remain unchanged. Purple block crystals were collected with the yield of 72.4 % (based on (based on cobalt)). Anal. Calcd for $\text{C}_{72}\text{H}_{56}\text{Co}_4\text{N}_{12}\text{O}_{20}$: C, 52.52; H, 3.40; N, 10.21 %. Found: C, 52.43; H, 3.51; N, 10.13 %. IR (KBr disk, cm^{-1}): 3126 (m), 3105 (m), 2929 (w), 1672 (s) 1627 (vs), 1599 (vs), 1570 (vs), 1500 (m), 1396 (vs), 1346 (s), 1313 (s), 1252 (s), 1095 (s), 1022 (w), 970 (m), 831 (m), 822 (m), 778 (m), 654 (m), 463 (w).

X-ray crystal structure determination

The suitable crystals of the coordination polymers were collected for single crystal X-ray diffraction. The data were collected on a Bruker Apex Smart CCD diffractometer, using graphite-monochromated Mo- α radiation ($\lambda = 0.71073 \text{ \AA}$) by the ω - 2θ scan mode. The structure was solved by direct methods using SHELXS-97. The non-hydrogen atoms were defined by the Fourier synthesis method. Positional and thermal parameters were refined by the full matrix least-squares method (on F^2) to convergence.

Electrochemical measurements

All electrochemical experiments were tested by CHI660E electrochemical analyzer. The test method for the electrochemical properties of MOFs in a weakly acidic condition is Linear Sweep Voltammetry (LSV), which was carried out in a single-chamber three-electrode electrolytic cell in which Ag/AgCl (saturated KCl solution) was used as a reference electrode;

a platinum wire electrode was used as a counter electrode; a F-doped tin oxide (FTO) conducting glass substrates (1 cm × 1 cm, active surface area was 1.0 cm²) was used as a working electrode (The working electrode should be washed alternately with absolute ethanol and deionized water, and dried); 0.1 mol·L⁻¹ of KH₂PO₄ was used as the electrolyte solution. Controlled-potential electrolysis (CPE) were performed with FTO glass electrode as the working electrode, which was obtained from Zhuhai Kaivo Optoelectronic Corp. A mixture of MOFs 1-3 (10 mg) and 3-4 drops of Nafion-ethanol (v/v = 1:9) was placed in a centrifuge tube, sonicated for 30 min, then applied to the FTO glass electrode surface. Before each experiment the solution was purged with high purity argon for 30 min. All the tests were carried out at room temperature.

Text S2. Adsorption isotherms

In order to designate the adsorption behavior and to assess the adsorption capacity, adsorption isotherms were studied by Langmuir and Freundlich isotherm models.

The non-linear expression of Langmuir isotherm model can be illustrated as:

$$q_e = qm \frac{K_L C_e}{1 + K_L C_e}$$

where C_e is the concentration of dyes at equilibrium; q_e is the corresponding adsorption capacity; qm and K_L are the constants related to the adsorption capacity and energy, respectively.

The important characteristic of the Langmuir isotherm can be expressed in terms of the dimensionless equilibrium parameter R_L , which is defined as:

$$R_L = \frac{1}{1 + bC_o}$$

It is considered to be a favorable adsorption process when the value of R_L is within the range of 0-1.0.

The Freundlich isotherm model assumes that the surface is heterogeneous and the energy of sorption is not constant. The non-linear form of Freundlich isotherm is expressed by the following equation:

$$q_e = K_F C_e^{1/n}$$

where K_f and n are the constants, which measure the adsorption capacity and intensity; respectively. The values of n represent deviation from linearity of adsorption process.

If $n = 1$ (linear adsorption process); $n < 1$ (chemical adsorption process); $n > 1$ (physical adsorption process).

Text S3. Adsorption kinetics models

The pseudo-first order equation is given as:

$$\ln(q_e - q_t) = \ln q_e - k_1 t$$

Where q_t is the adsorption capacity at time t ($\text{mg}\cdot\text{g}^{-1}$), and k_1 is the equilibrium rate constant (h^{-1}).

The pseudo-second order equation is given as:

$$\frac{t}{q_t} = \frac{1}{k_2 q_e^2} + \frac{t}{q_e}$$

Where q_t and q_e are the adsorption capacity at time t and equilibrium, respectively ($\text{mg}\cdot\text{g}^{-1}$); k_2 is the equilibrium rate constant ($\text{g}\cdot\text{mg}^{-1}\cdot\text{h}^{-1}$).

Text S4. Adsorption thermodynamic parameters

The thermodynamic parameters that are ΔH^0 (enthalpy change), ΔG^0 (standard free energy) and ΔS^0 (entropy change) for the adsorption of dyes onto MOFs **1-3** were calculated. The values of ΔH^0 and ΔS^0 were found from the slopes and intercepts of the plots of $\log K_c$ versus $1/T$ by using the equation:

$$\log k_c = -\frac{\Delta H^0}{2.303RT} + \frac{\Delta S^0}{2.303R}$$

$$\Delta G^0 = \Delta H^0 - T\Delta S^0$$

where R is the universal gas constant ($8.314 \text{ J}\cdot\text{mol}^{-1}\cdot\text{K}^{-1}$), T is the absolute temperature (K).

Table S1 Selected bond lengths (Å) and angles (°) for **1-3**

1			
Co1—O1	2.032 (3)	Co2—O2	2.035 (3)
Co1—O3	2.040 (3)	Co2—O4	2.009 (3)
Co1—O9 ⁱ	2.214 (3)	Co2—O5 ^{iv}	2.152 (3)
Co1—O10 ⁱ	2.127 (3)	Co2—O6 ^{iv}	2.177 (3)
Co1—N2 ⁱⁱ	2.148 (5)	Co2—N1	2.148 (4)
Co1—N3 ⁱⁱⁱ	2.158 (5)	Co2—N6 ^v	2.187 (5)
Co3—O12 ^{iv}	1.983 (3)	Co3—N4	2.053 (5)
Co3—O15	1.993 (4)	Co3—N8 ^{vi}	2.051 (4)
O1—Co1—O3	110.19 (13)	O3—Co1—O9 ⁱ	90.31 (12)
O1—Co1—O9 ⁱ	157.85 (13)	O3—Co1—O10 ⁱ	150.97 (13)
O1—Co1—O10 ⁱ	98.42 (13)	O3—Co1—N2 ⁱⁱ	98.22 (15)
O1—Co1—N2 ⁱⁱ	88.01 (16)	O3—Co1—N3 ⁱⁱⁱ	91.81 (15)
O1—Co1—N3 ⁱⁱⁱ	82.58 (16)	N2 ⁱⁱ —Co1—O9 ⁱ	97.52 (15)
O10 ⁱ —Co1—O9 ⁱ	60.67 (12)	N2 ⁱⁱ —Co1—N3 ⁱⁱⁱ	168.15 (15)
O10 ⁱ —Co1—N2 ⁱⁱ	87.33 (15)	N3 ⁱⁱⁱ —Co1—O9 ⁱ	88.68 (15)
O10 ⁱ —Co1—N3 ⁱⁱⁱ	86.93 (15)	O2—Co2—O5 ^{iv}	152.72 (12)
O2—Co2—O6 ^{iv}	92.18 (12)	O5 ^{iv} —Co2—O6 ^{iv}	60.67 (12)
O2—Co2—N1	96.14 (15)	O5 ^{iv} —Co2—N6 ^v	85.06 (14)

O2—Co2—N6 ^v	94.39 (14)	O5 ^{iv} —Co2—C5 ^{iv}	30.39 (14)
O2—Co2—C5 ^{iv}	122.56 (14)	O6 ^{iv} —Co2—N6 ^v	92.97 (14)
O4—Co2—O2	109.07 (13)	O6 ^{iv} —Co2—C5 ^{iv}	30.38 (14)
O4—Co2—O5 ^{iv}	98.17 (13)	N1—Co2—O5 ^{iv}	87.51 (14)
O4—Co2—O6 ^{iv}	158.64 (13)	N1—Co2—O6 ^{iv}	90.86 (14)
O4—Co2—N1	84.85 (15)	N1—Co2—N6 ^v	168.65 (15)
O4—Co2—N6 ^v	87.72 (15)	N1—Co2—C5 ^{iv}	87.26 (15)
O4—Co2—C5 ^{iv}	128.31 (14)	N6 ^v —Co2—C5 ^{iv}	90.65 (16)
O15—Co3—N4	126.90 (16)	O12 ^{iv} —Co3—O15	94.20 (14)
O15—Co3—N8 ^{vi}	102.35 (16)	O12 ^{iv} —Co3—N4	111.27 (16)
N8 ^{vi} —Co3—N4	113.99 (17)	O12 ^{iv} —Co3—N8 ^{vi}	104.75 (16)

Symmetry codes: (i) $x+1, y, z$; (ii) $-x+2, -y+1, -z+2$; (iii) $-x+1, -y+1, -z+1$;

2

Co1-N2 ⁱ	2.052 (2)	Co1-O1	2.029 (2)
Co1-O5 ⁱⁱ	2.230 (2)	Co1-N1 ⁱⁱⁱ	2.168 (3)
Co1-O4 ⁱⁱ	2.151 (2)	Co1-N2	2.122 (3)
O2 ⁱ —Co1—O5 ⁱⁱ	151.94 (9)	O1—Co1—O4 ⁱⁱ	152.06 (10)
O2 ⁱ —Co1—O4 ⁱⁱ	92.08 (9)	O1—Co1—N1 ⁱⁱⁱ	85.09 (10)
O2 ⁱ —Co1—N1 ⁱⁱⁱ	89.03 (10)	O1—Co1—N2	92.23 (11)
O2 ⁱ —Co1—N2	92.05 (11)	N1 ⁱⁱⁱ —Co1—O5 ⁱⁱ	93.83 (10)

O4 ⁱⁱ —Co1—O5 ⁱⁱ	60.08 (8)	N2—Co1—O5 ⁱⁱ	86.37 (10)
O4 ⁱⁱ —Co1—N1 ⁱⁱⁱ	89.43 (10)	N2—Co1—O4 ⁱⁱ	92.98 (10)
O1—Co1—O2 ⁱ	115.14 (10)	N2—Co1—N1 ⁱⁱⁱ	177.32 (10)
O1—Co1—O5 ⁱⁱ	92.92 (9)		

Symmetry codes: (i) -x+1, -y+1, -z+2; (ii) -x+1, -y, -z+2; (iii) x, y, z+1.

3

Co1—O2	1.915 (3)	Co1—N1	2.022 (4)
Co1—O4 ⁱ	1.980 (3)	Co1—N3 ⁱⁱ	2.053 (3)
O2—Co1—O4 ⁱ	128.74 (14)	O4 ⁱ —Co1—N1	98.41 (15)
O2—Co1—N1	110.46 (15)	O4 ⁱ —Co1—N3 ⁱⁱ	108.40 (14)
O2—Co1—N3 ⁱⁱ	104.39 (15)	N1—Co1—N3 ⁱⁱ	104.19 (15)

Symmetry codes: (i) -x+3/2, y-1/2, -z+3/2; (ii) -x+1/2, y-1/2, -z+3/2.

Thermogravimetric analysis (TGA) under dinitrogen in the range of 30-780 °C at a heating

rate of $10\text{ }^{\circ}\text{C min}^{-1}$ was carried out on **1-3** to investigate their thermal stability.

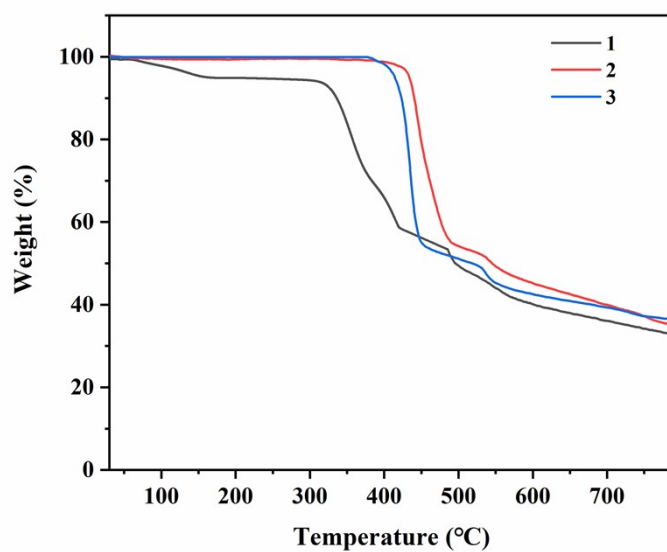


Fig. S1 TG curve of MOFs **1-3**.

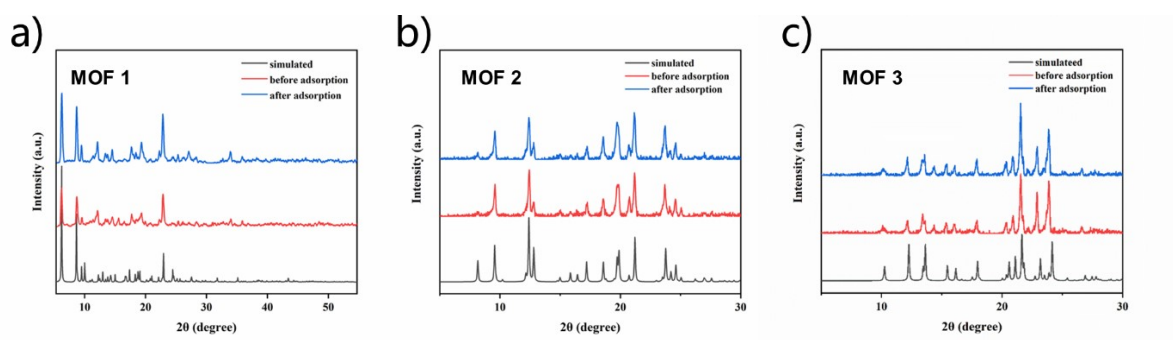


Fig. S2 The PXRD patterns of **1-3** before and after adsorption.

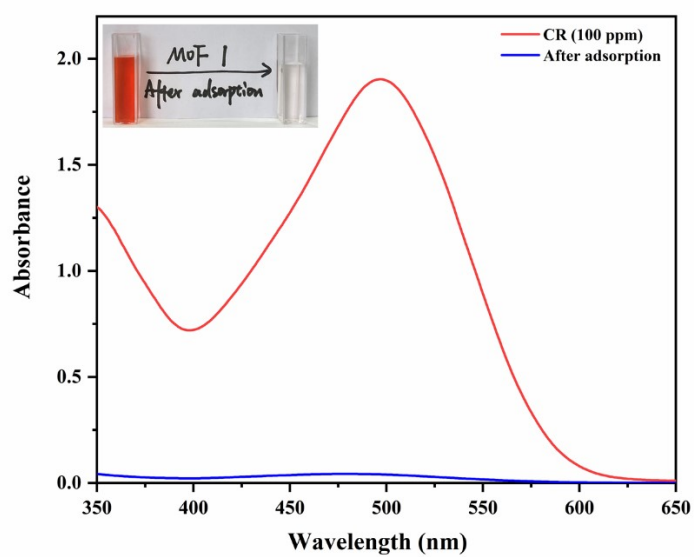


Fig. S3 Naked eye visualization of the adsorption of 100 ppm CR by **1** at room temperature and the corresponding UV-vis spectra of the solution.

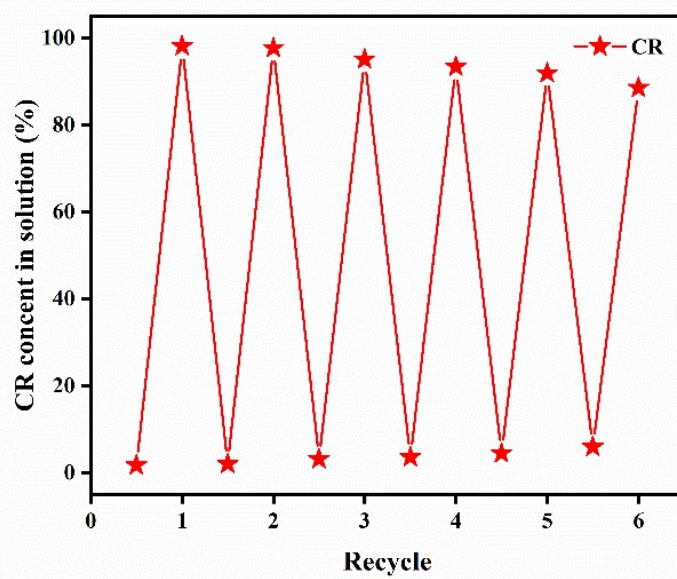


Fig. S4 The repeated adsorptions of CR for **1**.

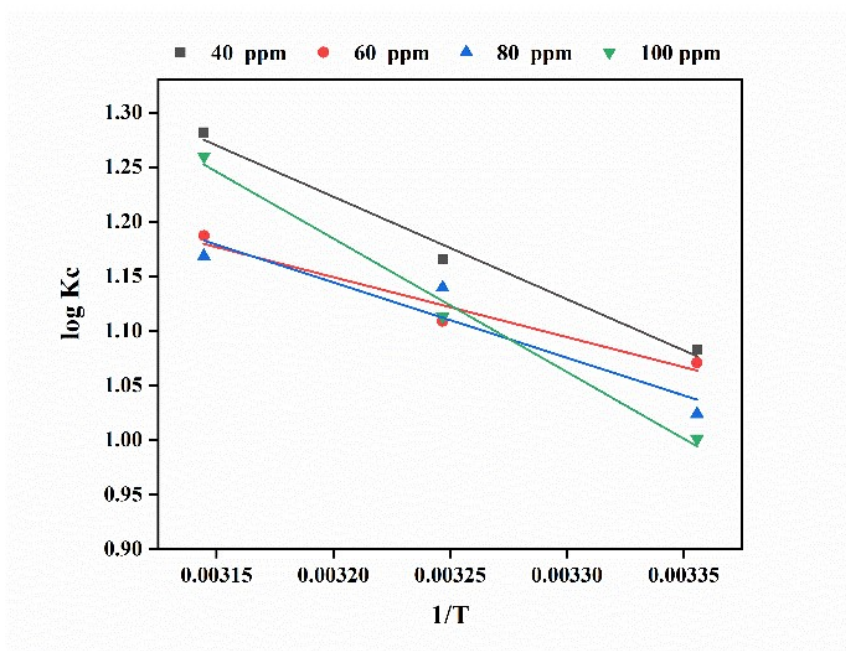


Fig. S5 Van't Hoff plots for the adsorption of CR dye onto **1**.

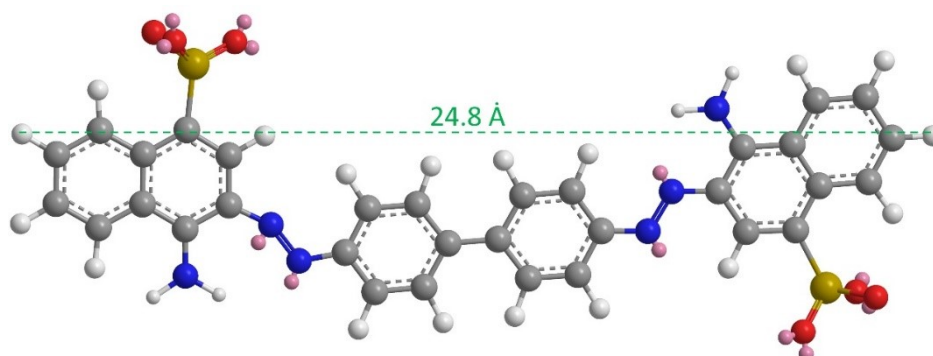


Fig. S6 Structural formula of congo red.

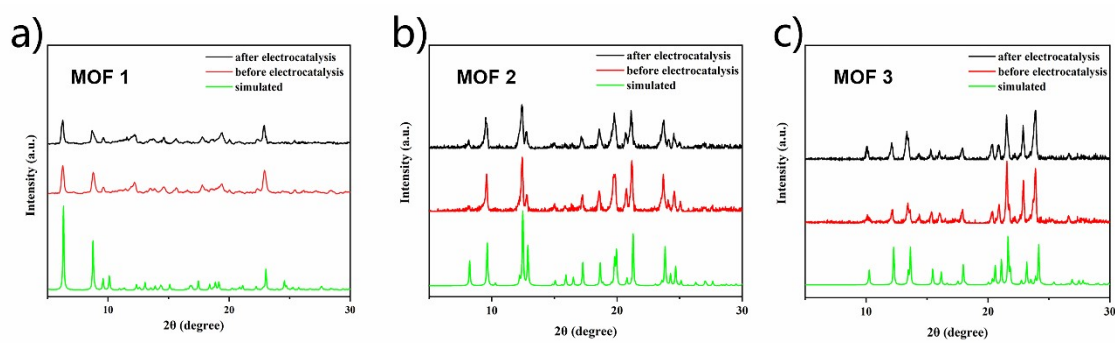


Fig. S7 The PXRD patterns of **1-3** before and after electrocatalysis.